Supporting Information for:

Planar Triangular Dy_3+Dy_3 Single-Molecule Magnet with a Toroidal Magnetic Moment

Experimental Section

General. All starting materials were of A.R. Grade and were used as commercially obtained without further purification. 4,6-dihydrazinopyrimidine was prepared according to a previously published method.[1]

Elemental analyses for C, H, and N were carried out on a Perkin-Elmer 2400 analyzer. Fourier transform IR (FTIR) spectra were recorded with a Perkin-Elmer FTIR spectrophotometer using the reflectance technique (4000−300 cm^{-1}). Samples were prepared as KBr disks. All magnetization data were recorded on a Quantum Design MPMS-XL7 SQUID magnetometer equipped with a 7 T magnet. The variable-temperature magnetization was measured with an external magnetic field of 1000 Oe in the temperature range of 1.9−300 K. The experimental magnetic susceptibility data are corrected for the diamagnetism estimated from Pascal's tables and sample holder calibration.

Synthesis of the Complex Dy_6[Br]

$[Dy_6L_2(\mu_3\text{-}OH)_4(\mu_2\text{-}OH)_2\ (H_2O)_{12}]\cdot 8Br\cdot 2CH_3CN\cdot 6CH_3OH$ (**Dy_6[Br]**).

4,6-dihydrazinopyrimidine (0.1 mmol) was dissolved in a mixture of methanol and acetonitrile (1:2, 15 mL), and then o-vanillin (0.2 mmol) was added to the mixture. The reaction mixture was stirred for 5 min. Then, KOH (0.2 mmol) and $DyBr_3\cdot 6H_2O$ (0.2 mmol) were added successively. The reaction mixture was stirred at room temperature for 3 h and the resultant solution was left unperturbed to allow for slow evaporation of the solvent. Yellow single crystals of complex **Dy_6[Br]** were obtained after about one week. Yield: 25 mg, (24.8 %, based on the metal salt). Elemental analysis (%) calcd for $C_{50}H_{96}Br_8Dy_6N_{14}O_{32}$: C, 19.89, H, 3.20, N, 6.49; found C, 19.85, H, 3.24, N, 6.55.

X-ray Crystallography.

Crystallographic data and refinement details are given in Table S1. Suitable single crystal of **Dy_6[Br]** was selected for single-crystal X-ray diffraction analysis. Crystallographic data were collected at

100(5) K on a Bruker ApexII CCD diffractometer and with graphite monochromated Mo Kα radiation (λ = 0.71073 Å). The structure was solved by direct methods and refined by the full-matrix least-squares method based on F^2 with anisotropic thermal parameters for all non-hydrogen atoms by using the SHELXS (direct methods) and refined by SHELXL (full matrix least-squares techniques) in the Olex2 package.[2] The locations of Dy and Br atoms were easily determined, and O, N, C atoms were subsequently determined from the difference Fourier maps. Anisotropic thermal parameters were assigned to all non-hydrogen atoms. The H atoms were introduced in calculated positions and refined with a fixed geometry with respect to their carrier atoms. CCDC 1445859 (**Dy_6[Br]**) contains the supplementary crystallographic data for this paper. This data can be obtained free of charge from the Cambridge Crystallographic Data Centre via www.ccdc.cam.ac.uk/data_request/cif.

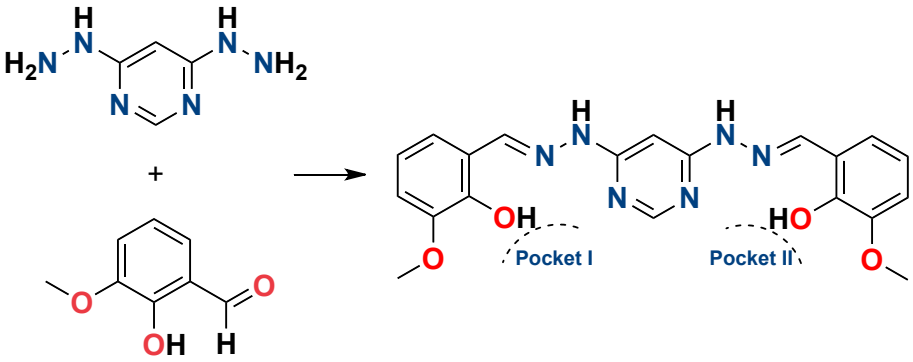

Scheme S1. Structure of the H_2L ligand and two coordination pockets.

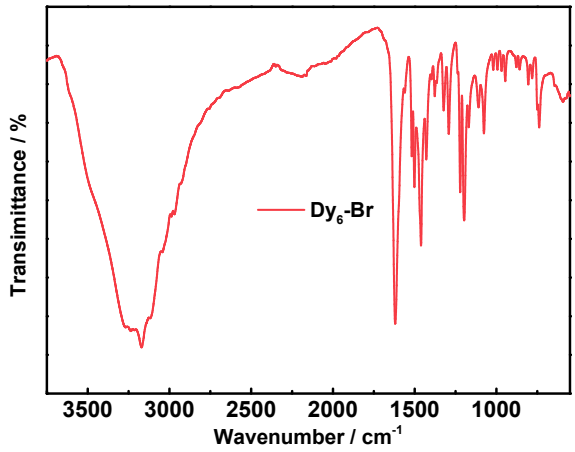

Fig. S1. IR spectrum of a crystalline sample of complex **Dy_6[Br]**.

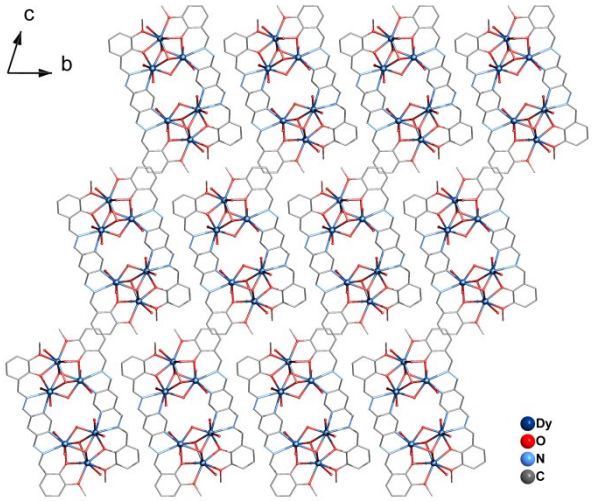

Fig. S2. Crystal packing of complex **Dy_6[Br]** along *a* axis.

Table S1. Crystal data and structure refinement for **Dy_6[Br]**.

Compound	**Dy_6[Br]**
Empirical formula	$C_{50}H_{96}Br_8Dy_6N_{14}O_{32}$
Formula weight	3019.68
Temperature/K	100(2)
Crystal system	triclinic
Space group	P-1
a/Å	11.225(2)
b/Å	12.338(2)
c/Å	18.269(3)
α/°	72.433(3)
β/°	82.638(4)
γ/°	89.180(4)
V/Å^3	2391.5(7)
Z	1
μ/mm^{-1}	8.047
F(000)	1462.0
R_{int}	0.0400
GoF	1.042
*R_1 wR_2 [$I >= 2\sigma(I)$]	0.0851, 0.2260
*R_1 wR_2 [all data]	0.1206, 0.2555

*$R1 = \Sigma||Fo| - |Fc||/\Sigma|Fo|$ for $Fo > 2\sigma(Fo)$; $wR2 = (\Sigma w(Fo^2 - Fc^2)^2/\Sigma(wFc^2)^2)^{1/2}$ all reflections, $w = 1/[\sigma^2(Fo^2)+(0.1557P)^2]$ where $P = (Fo^2+2Fc^2)/3$

Table S2. Dy^{III} geometry analysis of **Dy_6[Br]/Dy_6−SCN**[3] by SHAPE 2.1 software.[4]

Dy^{III}	**TDD-8** (***D_{2d}***)	**SAPR-8** (***D_{4d}***)	**BTPR-8** (***C_{2v}***)	**JBTPR-8** (***C_{2v}***)	**JSD-8** (***D_{2d}***)
Dy^{III}(1)	1.930/1.982	1.382/1.418	2.786/2.844	3.322/3.525	5.021/4.981
Dy^{III}(2)	0.973/0.840	2.303/3.005	1.848/2.315	2.221/2.596	2.024/2.057
Dy^{III}(3)	0.869/1.008	2.790/2.539	1.868/1.887	2.246/2.342	1.889/2.102

TDD-8 = Triangular dodecahedron; SAPR-8 = Square antiprism; BTPR-8 = Biaugmented trigonal prism; JBTPR-8 = Biaugmented trigonal prism J50; JSD-8 = Snub diphenoid J84.

Table S3. The corresponding distances and angles of Dy_3 triangle in complexes **Dy_6[Br]**, **Dy_6−NO_3** and **Dy_6−SCN**.[3]

	Dy_6[Br]	**Dy_6−NO_3**	**Dy_6−SCN**
Dy1−Dy2	3.510 Å	3.523 Å	3.540 Å
Dy1−Dy3	3.509 Å	3.512 Å	3.534 Å
Dy2−Dy3	3.486 Å	3.519 Å	3.505 Å
Dy1−Dy2−Dy3	60.207°	59.835°	60.206°
Dy2−Dy3−Dy1	60.239°	60.142°	60.390°
Dy3−Dy1−Dy2	59.554°	60.023°	59.403°
Dihedral Angle	0°	0°	5.153°
Distance between two Dy_3 plans	0.2610 Å	0.2361 Å	–

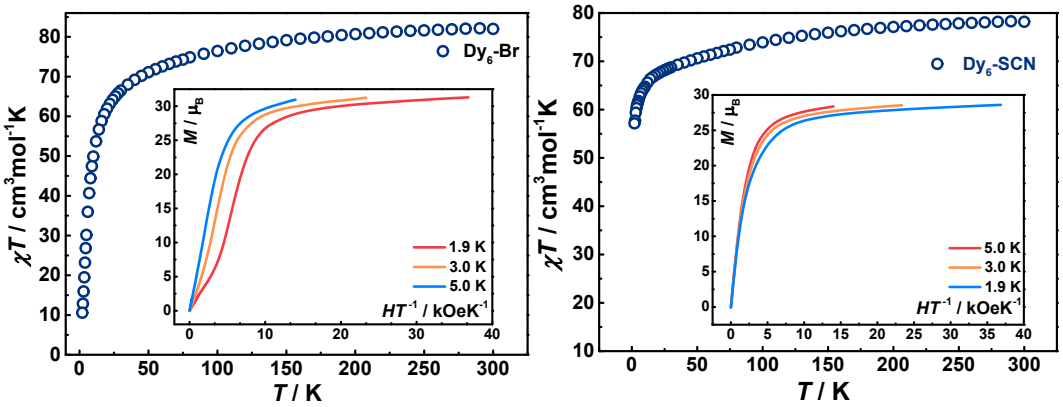

Fig. S3. Temperature dependence of the $\chi_M T$ products for **Dy$_6$[Br]** (left) and **Dy$_6$−SCN** (right). Insets: *M vs*. *H*/*T* plots for **Dy$_6$[Br]** and **Dy$_6$−SCN**.[3]

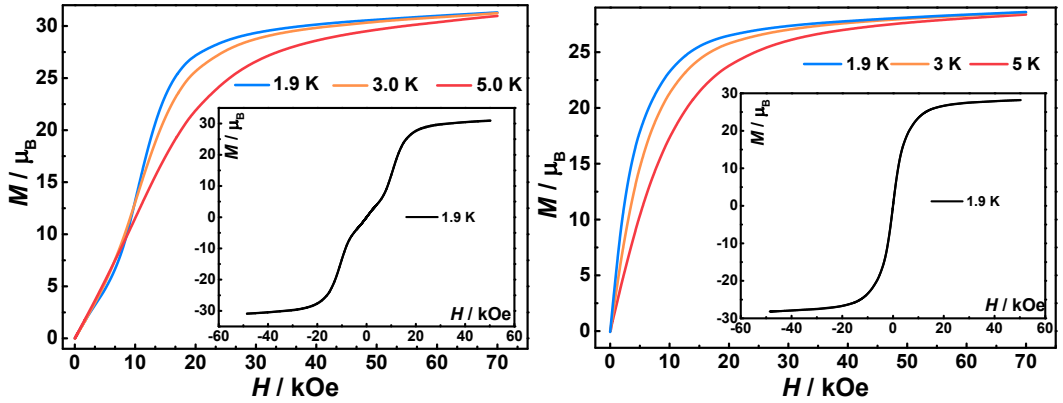

Fig. S4. Plots of the reduced magnetization *M* versus *H* in the field range 0−70 kOe and temperature range 1.9−5.0 K for **Dy$_6$[Br]** (left) and **Dy$_6$−SCN** (right). Insets: Hysteresis loops for complexes **Dy$_6$[Br]** and **Dy$_6$−SCN**[3] at 1.9 K.

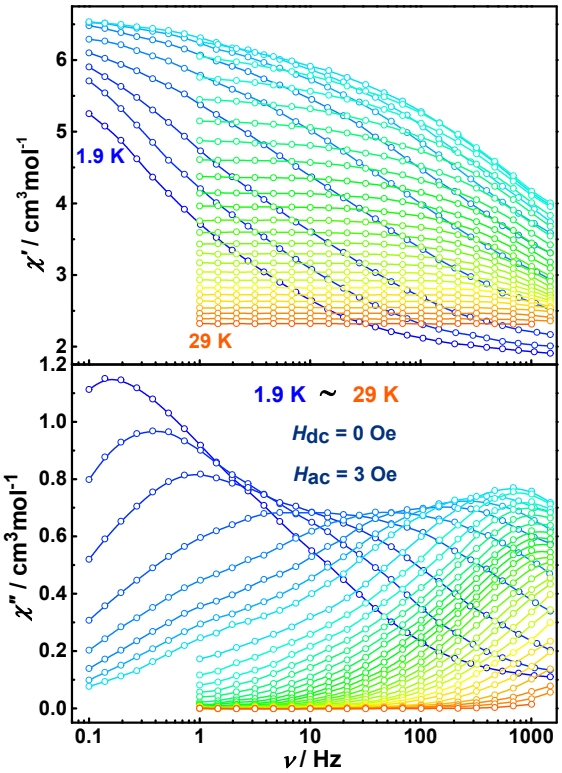

Fig. S5. Frequency dependence of the in-phase (χ') and out-of-phase (χ'') ac susceptibility signals between 1.9 and 29 K for **Dy_6[Br]** under zero dc-field. The Solid lines are guides for the eye.

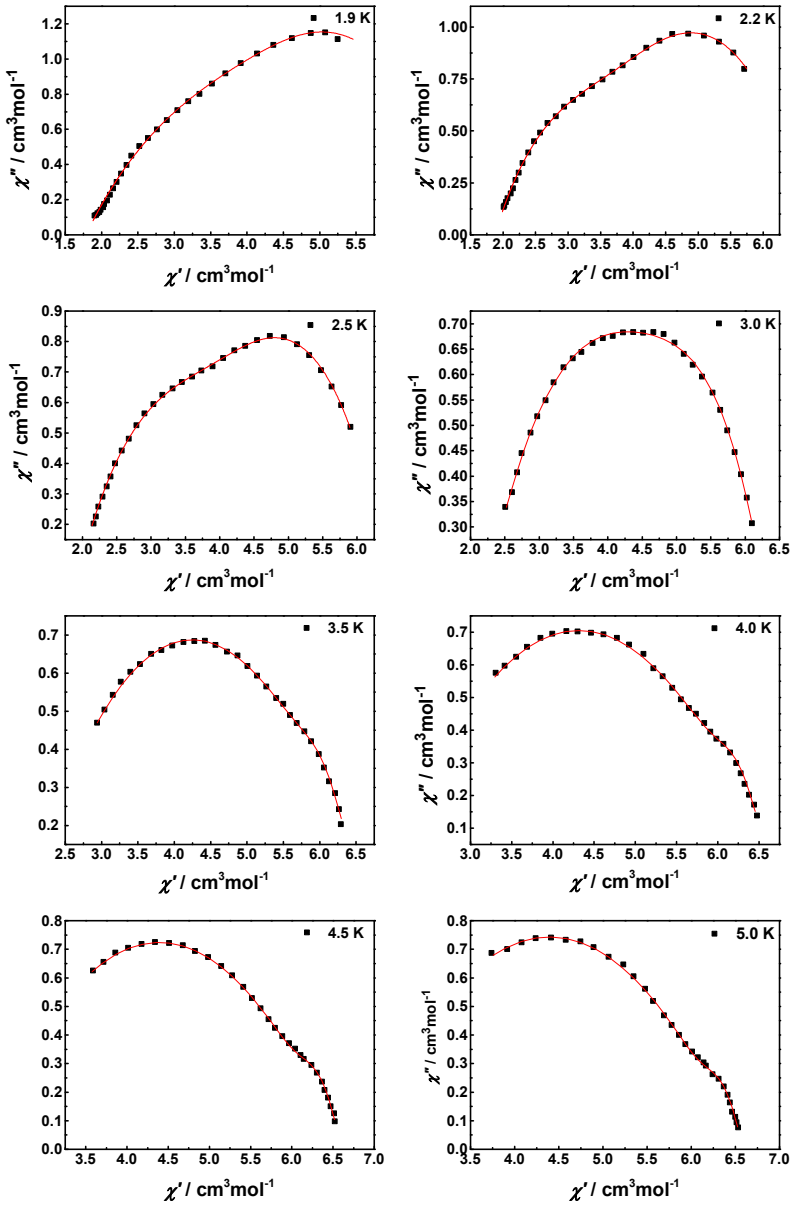

Fig. S6. Simulations of dynamical susceptibility $\chi(\omega)$ ranging from 1.9 to 5.0 K in a Cole-Cole diagram. Red lines were performed using the sum of two modified Debye functions with the fitting parameters in Table S4.

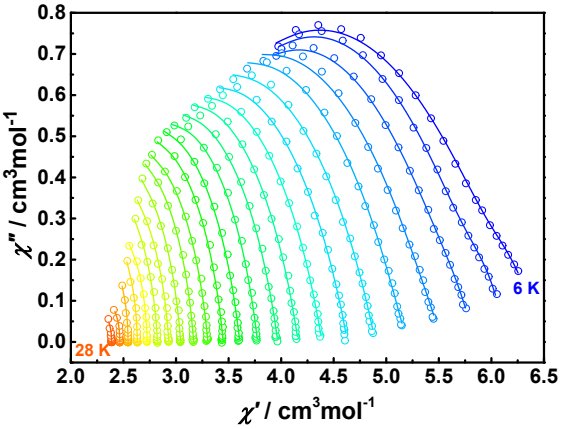

Fig. S7. Cole−Cole plots for temperatures between 6.0 and 28 K under a zero dc field with the best fit to the generalized Debye model for **Dy_6[Br]**. The Solid lines represent fits to the data, as described in the main text.

Table S4. Relaxation fitting parameters for Cole−Cole plots of **Dy_6[Br]** at varying temperatures under zero applied dc-field using the sum of two modified Debye model.[5]

T (K)	$\chi_{S,tot}$	$\Delta\chi_1$	$\Delta\chi_2$	α_1	α_2
1.9	1.78461	1.17309	4.16368	0.11836	0.54831
2.2	1.87779	2.44629	2.30855	0.30245	0.47798
2.5	1.93592	2.42840	2.04991	0.496238	0.337360
3.0	2.00447	3.14440	1.30382	0.560090	0.408852
3.5	2.00027	4.47238	1.43542	0.621028	0.544831E-05
4.0	2.14493	4.32320	1.71629	0.598797	0.929027E-05
4.5	2.32686	4.12037	1.82288	0.570140	0.138736E-04
5.0	2.34600	4.09086	1.66834	0.556613	0.191979E-04

$$\chi_{AC}(\omega) = \chi_{S,tot} + \frac{\Delta\chi_1}{1+(i\omega\tau_1)^{(1-\alpha_1)}} + \frac{\Delta\chi_2}{1+(i\omega\tau_2)^{(1-\alpha_2)}} \qquad \text{(S1)}$$

Table S5. The best fitting parameters for Cole−Cole plots of **Dy_6[Br]** at varying temperatures under zero applied dc field.

T (K)	χ_T	χ_S	α
6.0	6.43245	1.93195	0.583408
7.0	6.14763	2.05519	0.551422
8.0	5.82471	2.21641	0.516488
9.0	5.50205	2.12184	0.494872
10	5.18226	2.21604	0.451108
11	4.89571	2.21726	0.425339
12	4.63123	2.24005	0.392210
13	4.38814	2.22535	0.359684
14	4.16152	2.17889	0.330333
15	3.96813	2.13623	0.309396
16	3.77588	2.14245	0.268330
17	3.60639	2.04133	0.259611
18	3.44900	2.03767	0.226546
19	3.30268	1.99495	0.215094
20	3.16781	1.97049	0.182911
21	3.04430	1.89804	0.181636
22	2.93196	1.92896	0.165964
23	2.82413	1.93778	0.137054

Computational details. Wave-function-based calculations were carried out on three models (see below and Figure S8) of **Dy_6[Br]**, **Dy_6-SCN** and **Dy_6-NO_3** by using the CASSCF/SI-SO approach, as implemented in the MOLCAS quantum chemistry package (version 8.0).[6] Coordinates were extracted from X-ray crystal structures. Relativistic effects are treated in two steps on the basis of the Douglas–Kroll Hamiltonian. First, the scalar terms were included in the basis-set generation and used to determine the spin-free wave functions and energies in the complete active space self-consistent field (CASSCF) method.[7] Next, spin–orbit coupling was added within the restrict- ed active space state interaction (RASSI-SO) method, which uses the spin-free wave functions as basis states.[8] The resulting wave functions and energies are used to compute the magnetic proper- ties and g tensors of the lowest states from the energy spectrum by using the pseudospin S = 1/2 formalism in the SINGLE-ANISO routine.[9] Magnetic coupling constants were obtained by using the POLY_ANISO routine by comparison with experimental magnetic data.[9,10] For each complex, even if Dy centers are not equivalent, only one exchange coupling was considered when fitting the experimental magnetic data. Cholesky decomposition of the bielectronic integrals was employed to

save disk space and speed up the calculations.[11] The models used consist in only half of the **Dy_6** molecule taking advantage of the centrosymmetry (Figure S8). To investigate the local properties of each Dy^{III} ion, other two Dy^{III} ions were replaced by the closed-shell Y^{III} ion. The active space of the CASSCF method consisted of the nine 4f electrons of the Dy^{III} ion spanning the seven 4f orbitals, that is, CAS(9,7)SCF. State-averaged CASSCF calculations were performed for all of the sextets (21 roots), all of the quadruplets (224 roots), and 300 out of the 490 doublets (due to software limitations) of the Dy^{III} ion. 21 sextets, 128 quadruplets, and 107 doublets were mixed through spin–orbit coupling in RASSI-SO. All atoms were described by ANO-RCC basis sets.[12] The following contractions were used: [8s7p4d3f2g1h] for Dy, [7s6p4d2f] for Y, [4s3p2d] for O and N directly coordinated to Dy (for all O in the case of **Dy_6-NO_3**), [4s3p] for S, [3s2p] for C and the other O and N atoms, and [2s] for the H atoms.

Table S6. Ab initio energies (cm^{-1}) of the Kramers doublet, g tensors and orientation of the anisotropy axes for the ground Kramers doublet of each of the three dysprosium ions in **Dy_6[Br]**, **Dy_6-SCN** and **Dy_6-NO_3**.

	Dy_6[Br]			**Dy_6-SCN**			**Dy_6-NO_3**		
	Dy1	Dy2	Dy3	Dy1	Dy2	Dy3	Dy1	Dy2	Dy3
KD1	0	0	0	0	0	0	0	0	0
KD2	208	211	199	88	141	165	130	129	170
KD3	291	263	255	108	169	184	178	166	257
KD4	341	329	307	170	196	222	223	248	280
KD5	397	373	358	228	256	294	267	297	317
KD6	434	429	394	292	308	348	295	310	356
KD7	515	464	424	362	375	392	327	337	404
KD8	530	615	608	389	419	476	440	379	483
	g tensors of the lowest KD								
g_x	0.00	0.00	0.01	0.03	0.01	0.02	0.07	0.03	0.00
g_y	0.00	0.00	0.01	0.06	0.02	0.03	0.16	0.06	0.01
g_z	19.75	19.68	19.67	19.43	19.63	19.66	19.49	19.58	19.77
	Tilted angle between anisotropy axis and the tangential direction								
	2.9	-9.7	6.9	-	-11.0	14.7	1.9	-13.6	14.6
	Tilted angle between anisotropy axis and the Dy_3 plane								
	7.0	-3.2	3.2	81.3	0.6	-3.0	0.7	3.8	3.0

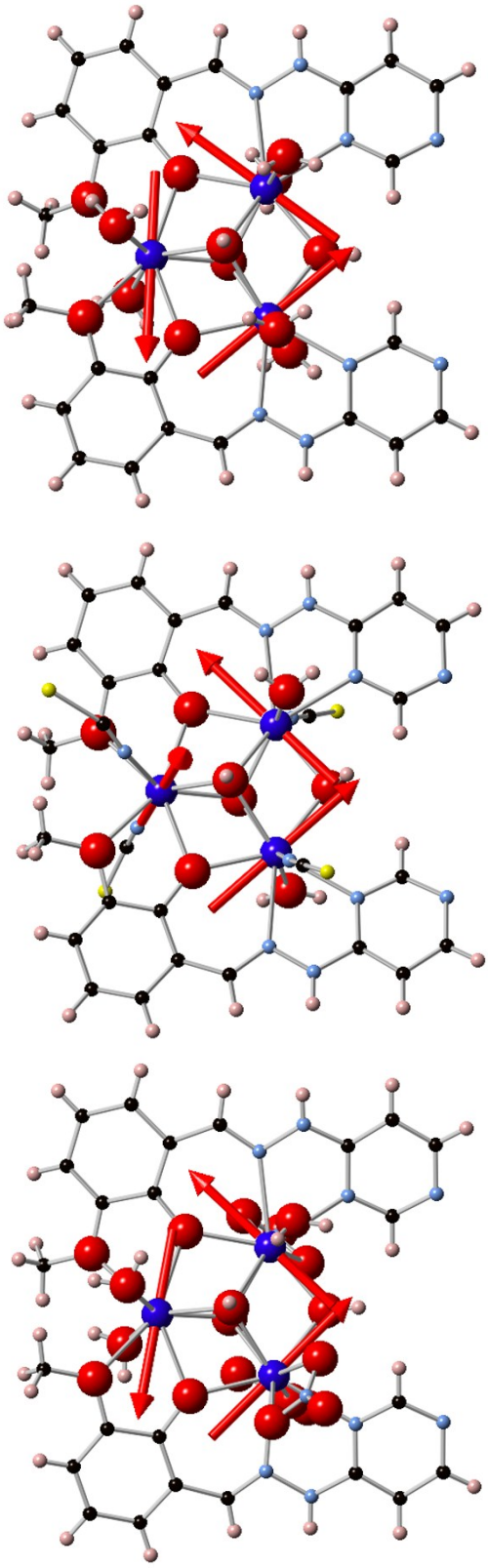

Fig. S8. Dy_3 model used in the calculations for **Dy_6[Br]** (top), **Dy_6-SCN** (middle) and **Dy_6-NO_3** (bottom) with the calculated local anisotropy axes of the ground KD on each Dy(III) ion. Color scheme: Dy, blue; O, red; N, light blue; C, black; S, yellow; H, grey. Label of Dy(III) ions are: Dy1, left; Dy2, bottom; Dy3, top.

Table S7. Exchange coupling and dipolar interactions (in cm^{-1}) calculated in **Dy_6[Br]**, **Dy_6-SCN** and **Dy_6-NO_3**. For the dipolar interactions, only the zz component is considered but all terms were included in the POLY_ANISO calculations.

Dy_6[Br]			**Dy_6-SCN**[b]			**Dy_6-NO_3**		
Exchange coupling constants[a]								
-7.5			-16.25			5.0		
Dy1-Dy2	Dy1-Dy3	Dy2-Dy3	Dy1-Dy2	Dy1-Dy3	Dy2-Dy3	Dy1-Dy2	Dy1-Dy3	Dy2-Dy3
Dipolar interactions								
-1.48	-1.54	-1.81	-0.09	-0.02	-3.08	-1.43	-1.39	-1.89
Total magnetic interactions								
-8.98	-9.04	-9.31	-16.34	-16.27	-19.33	3.57	3.61	3.11

[a] the exchange coupling parameters were obtained within Lines model and then written in the Ising model. [b] the obtained interactions clearly show the limits of a single-parameter for the exchange interaction in the case of **Dy_6-SCN**. This is in line with the orientation of the local anisotropy axis calculated for Dy1 in this complex.

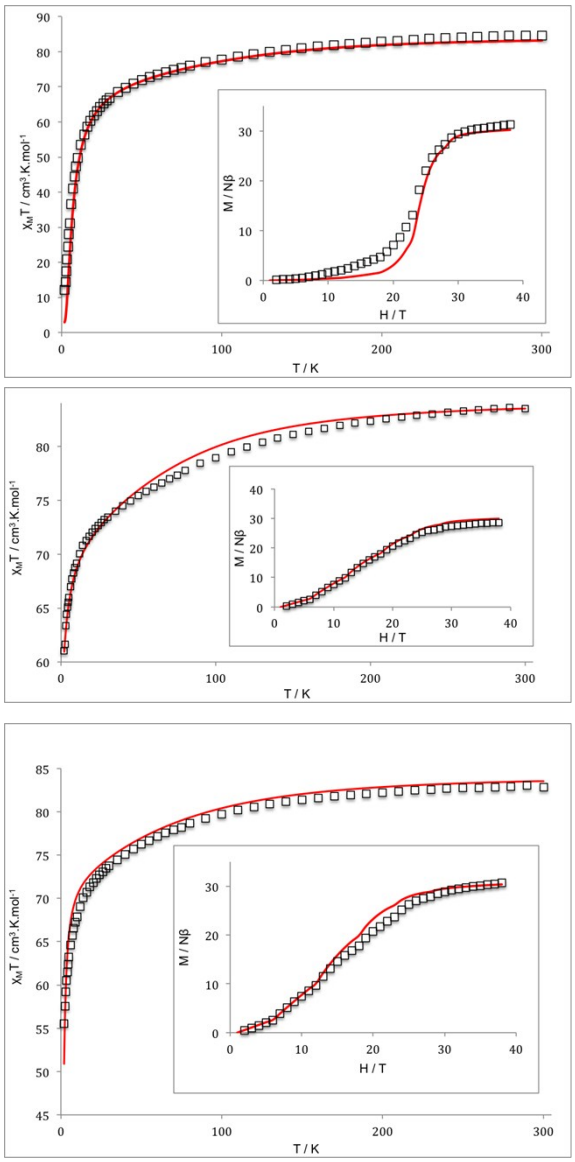

Fig. S9. Experimental and simulated (using magnetic interactions given in Table S7) temperature dependence of the $\chi_M T$ product and magnetization at 1.9 K for **Dy_6[Br]** (top), **Dy_6-SCN** (middle) and **Dy_6-NO_3** (bottom).

References

1 V. P. K. M. B. Bushuev, N. V. Semikolenova, Yu. G. Shvedenkov,L. A., G. G. M. Sheludyakova, L. G. Lavrenova, V. A. Zakharov, and S. V. and Larionov, *Russ. J. Coord. Chem.*, 2007, **33**, 601.

2 (a) G. M. Sheldrick, *Acta Crystallogr. A*, 2008, **64**, 112; (b) O. V. Dolomanov, L. J. Bourhis, R. J. Gildea, J. A. K. Howard and H. Puschmann, *J. Appl. Crystallogr.*, 2009, **42**, 339.

3 X. L. Li, H. Li, D. M. Chen, C. Wang, J. Wu, J. Tang, W. Shi and P. Cheng, *Dalton Trans.*, 2015, **44**, 20316.

4 D. Casanova, M. Llunell, P. Alemany and S. Alvarez, *Chem. Eur. J.*, 2005, **11**, 1479.

5 Y.-N. Guo, G.-F. Xu, Y. Guo and J. Tang, *Dalton Trans.*, 2011, **40**, 9953.

6 F. Aquilante, L. De Vico, N. Ferré, G. Ghigo, P.-A. Malmqvist, P. Neogrady, T. Bondo Pedersen, M. Pitonak, M. Reiher, B. O. Roos, L. Serrano-Andrés, M. Urban, V. Veryazov, R. Lindh, *J. Comput. Chem.* 2010, **31**, 224.

7 B. O. Roos, P. R. Taylor, P. E. M. Siegbahn, *Chem. Phys.* 1980, **48**, 157.

8 (a) P.-A. Malmqvist, B. O. Roos, B. Schimmelpfennig, *Chem. Phys. Lett.* 2002, **357**, 230; (b) P.-A. Malmqvist, B. O. Roos, *Chem. Phys. Lett.* 1989, **155**, 189.

9 L. Chibotaru, L. Ungur, A. Soncini, *Angew. Chem. Int. Ed.* 2008, **47**, 4126.

10 (a) L. Ungur, W. Van den Heuvel and L. F. Chibotaru, New J. Chem., 2009, 33, 1224 ; (b) L. Ungur and L. F. Chibotaru, in Lanthanides and Actinides in Molecular Magnetism, Wiley-VCH Verlag GmbH & Co. KGaA, 2015, pp. 153–184.

11 F. Aquilante, P.-A. Malmqvist, T. B. Pedersen, A. Ghosh, B. O. Roos, *J. Chem. Theory Comput.* 2008, **4**, 694.

12 (a) B. O. Roos, R. Lindh, P.-A. Malmqvist, V. Veryazov, P.-O. Widmark, *J. Phys. Chem. A* 2004, **108**, 2851; (b) B. O. Roos, R. Lindh, P.-A. Malmqvist, V. Veryazov, P.-O. Widmark, *J. Phys. Chem. A* 2005, **109**, 6576; (c) B. O. Roos, R. Lindh, P.-A. Malmqvist, V. Veryazov, P.-O. Widmark, A. C. Borin, *J. Phys. Chem. A* 2008, **112**, 11431.